Chapter 10

Vibrational Spectroscopy for Quality Assessment of Meat

Ana M. Herrero[1], Pedro C. Hernandez[2], Francisco Jiménez-Colmenero[1] and Claudia R.-C. Perez[1]

[1]Institute of Food Science, Technology and Nutrition (ICTAN-CSIC), Madrid, Spain, [2]Institute of the Structure of Matter (CSIC), Madrid, Spain

10.1 INTRODUCTION

Meat is a rich nutrient matrix with high-value dietary components and generally meat demand and consumption is very high in most countries. Although, during recent years, a modest and decelerating growth in world per capita consumption of meat has been taking place, the world meat economy has been characterized by the rapid growth of the poultry sector (FAO, 2012). In fact, in developing countries, where almost all world population increases take place, it is estimated that meat consumption will increase considerably to 9 kg in 2030 and to 18 kg in 2050, of which 12.5 kg will be poultry meat (FAO, 2012).

Meat is a very heterogeneous product since the chemical composition, technological and sensory attributes are highly influenced by several factors. Meat quality is a result of complex interactions between the biological traits of the live animal and biochemical processes that occur postmortem as muscle is converted to meat, preserved and consumed (Jimenez-Colmenero et al., 2016). The variability in meat quality stems from several factors (including those relating to species) that arise throughout the production chain; therefore, it is the main concern of the industry (producers and manufacturers), distributors, retailers, consumers, and authorities. In this context, interest is centered on establishing the most effective methods of assessing the quality of meat and meat products. Traditionally, for evaluation of meat quality, sensory and microbiological analysis has been used as well as certain physicochemical methods (texture, water binding properties, color, etc.). Nevertheless, most of these traditional quality methods are time consuming and destructive, and it is not possible to apply them online during handling, processing, and storage. These are the main reasons why, in the last few

Poultry Quality Evaluation. DOI: http://dx.doi.org/10.1016/B978-0-08-100763-1.00010-6
© 2017 Elsevier Ltd. All rights reserved.

years, great efforts have been made in order to improve the methodology for the measurement of the objective quality of meat, in order to identify methods that solve all the disadvantages of the traditional methodology and may become sufficiently robust, rapid, and nondestructive or noninvasive for the quality assessment of meat. In this respect, the use of vibrational spectroscopic techniques (infrared (IR) and Raman spectroscopy) have several advantages compared to the traditional methods, due to the fact that they are direct, nondestructive or noninvasive, and their application in situ is possible (Damez and Clerjon, 2008; Herrero, 2008a; Prieto et al., 2009; Herrero et al., 2010). This is the reason why vibrational spectroscopic techniques have increased their importance in the determination of meat quality. Therefore, the purpose of this chapter is to provide insights into the study of structural features of meat components such proteins, lipids, and water using vibrational spectroscopic techniques. Additionally, the aim of this chapter is to cover aspects of the applications of these spectroscopic techniques (IR and Raman spectroscopy) as tools for meat quality assessment.

10.2 STRUCTURAL CHARACTERISTICS OF PROTEINS, LIPIDS, AND WATER DETERMINED BY VIBRATIONAL SPECTROSCOPY

10.2.1 Basic Spectroscopic Concepts

Vibrational spectroscopy, which includes IR and Raman spectroscopies, is based on the transitions between quantized vibrational energy states of molecules. In IR spectroscopy, the energy for these transitions is provided by radiation in the IR regions (near-IR and mid-IR) of the electromagnetic spectrum (Schrader, 1995). Transmission is the most powerful method that is well-suited to liquids and gases, and reflection spectroscopy offers the alternative that is almost always used in meat science. A remarkable increase of mid-IR applications has been produced as a result of the development of mid-IR Fourier transform (FT-IR) spectrometers in conjunction with sampling techniques including attenuated total reflection (ATR), for solids, semisolids, and liquids, due to the advantages offered (Li-Chan, 2010). Additionally, FT-IR microscopes have opened up new applications for in situ microspectroscopic mapping and imaging of food (Sedman et al., 2010). In recent years, the hyperspectral imaging (HSI) technique has emerged as a smart and promising analytical tool for quality-evaluation purposes and has attracted much interest in the nondestructive analysis of different food products. The main inducement for developing the HSI system is to integrate both spectroscopy (mainly near-IR spectroscopy (NIR)) and imaging techniques in one system to make direct identifications of different components and their spatial distributions in the tested products (ElMasry et al., 2012a, 2012b; Xiong et al., 2015). By combining spatial and spectral details, HSI

has proved to be a promising technology for objective meat quality evaluation.

In Raman spectroscopy, samples are excited with a source of monochromatic incident radiation that may be in the ultraviolet (UV), visible (VIS), or NIR regions of the electromagnetic spectrum (Schrader, 1995). In food, visible Raman radiation can be masked by fluorescence. However, Fourier transform Raman spectroscopy (FT-Raman), using NIR excitation from a Nd: YAG laser at 1064 nm, can generally avoid the problem of fluorescence (Li-Chan, 2010). Techniques such as surface-enhanced Raman spectroscopy (SERS), confocal Raman microspectroscopy, and Raman imaging spectroscopy are recognized for their potential and specific advantages in studying food components at very low concentrations, and for in situ multicomponent analysis.

Complementary information on fundamental vibrational modes can be obtained from mid-IR and Raman spectra, as some vibrational motions are detected primarily with IR radiation and others primarily by Raman scattering. Vibrational spectroscopy in particular offers many advantages in food studies (Li-Chan, 1996; Herrero, 2008a,b; Damez and Clerjon, 2008; Cozzolino, 2015; Cheng and Sun, 2015; Santos et al., 2015). Raman and IR spectroscopy can be applied to condensed-phase samples in various physical states, whether liquid or solid, clear or opaque. In many cases, minimal or no sample preparation or pretreatment is required, and a vibrational spectrum can usually be acquired within a relatively short time (Chalmers and Griffiths, 2007).

10.2.2 Spectral Analysis of Complex Biological Systems

Conventional IR and Raman spectroscopies are informative for studying the molecular structure of biological materials and for qualitative and quantitative applications. However, because of the molecular complexity of food which involves band overlapping, it is hard to extract useful detailed information from the spectral data. In order to better identify the individual components and maximize their response, the spectra can be analyzed by two basic techniques, namely, second-derivative formation and self-deconvolution. Second-derivative formation of a spectral contour clearly detects variations in the band components. Self-deconvolution is an artificial resolution enhancement. Both mathematical procedures allow the detection of spectral contributions in an overlapped band spectral profile (Surewicz and Mantsch, 1984). The resulting bands obtained by resolution enhancement (or by second-derivative formation) can subsequently be used to describe the measured spectral envelope by individual band components. These can be used then with aims of quality inspection by using multivariate analysis, e.g., discriminant analysis, receiver-operating characteristic analysis (ROC curves), etc.

10.2.2.1 Two-Dimensional Correlation Spectroscopy

Two-dimensional correlation spectroscopy (2D-COS) is another powerful technique which can be useful for spectral analysis of complex biological systems, such as food (Noda, 2007). This 2D correlation analysis allows the correlation of the dynamic fluctuations of either IR or Raman bands in a series of spectra measured at different times during application of an external perturbation, which can be temperature, pressure, concentration, isotopic exchange, etc.

Cross-correlation analysis provides 2D spectra that are defined by two independent frequencies, ν_1 (abscissa) and ν_2 (ordinate). The synchronous 2D correlation spectra of dynamic spectral intensity variations represent the simultaneous occurrence of coincidental changes in spectral intensities measured at ν_1 and ν_2. Correlation peaks appear at both diagonal (auto-peaks) and off-diagonal peaks (cross-peaks). Cross-peaks, which can either be positive or negative, reflect correlated changes of functional groups within the biomolecular system that occur simultaneously in the same (+) or in the opposite (−) direction. By contrast, the asynchronous 2D correlation representation is characterized by missing autopeaks and asymmetric cross-peaks which reveal uncorrelated (i.e., out-of-phase) behavior of two bands. The time-dependent changes in the spectral intensities are shown as 2D contours, called synchronous and asynchronous maps (S- and A-maps), which correlate to in-phase (synchronized) and out-of-phase (unsynchronized) intensity changes at two frequencies, respectively. Cross-peaks, which occur in both the S- and A-maps, provide information about the temporal order of the spectral changes. Cross-peaks with the same sign in the S- and A-maps indicate that a spectral change of the ν_1 band (abscissa) occurs predominantly before that of the ν_2 (ordinate) band in the sequential order of time. The temporal order is reversed for opposite signs of the S- and A-map cross-peaks.

The advantages of this technique, as compared with 1D vibrational spectroscopy, are summarized as follows: (1) enhancement of apparent spectral resolution of overlapped bands; (2) band assignments through observations of correlations between the bands; (3) studies of inter- and intra-molecular interactions through selective correlation between bands; and (4) probing the specific order in which the intensities of various bands change during application of an external perturbation.

In particular, 2D-COS visible/near-IR analysis has been used to study the thermal processing of chicken meat (Liu et al., 2000). The synchronous map revealed that at least two bands around 445 and 560 nm decreased in intensity with cooking time, which may be assigned to deoxymyoglobin and oxymyoglobin, respectively. The asynchronous 2D-NIR correlation map indicated that C−H fractions were easily oxidized. The effect of cold storage on chicken meat was also studied using generalized 2D visible/NIR correlation spectroscopy (Liu and Chen, 2000). The 2D correlation analysis in the

NIR region indicated that the change in O−H/N−H bands occurred before the change in C−H groups during cold storage. This revealed that during cold storage, water species interacted with other meat components, and this interaction could lead to proteolysis and denaturation of meat proteins, which is associated with the development of tenderization during storage (aging) (Liu and Chen, 2000). From the asynchronous correlation analysis in the visible and NIR regions, the authors concluded that chicken meat discoloration occurred earlier than other developments, such as the tenderization process (Liu and Chen, 2000). Subsequently, the same authors studied the thawing behavior of frozen chicken meat using generalized 2D visible/NIR correlation spectroscopy (Liu and Chen, 2001). The study was carried out when the frozen chicken meat was tightly covered by a quartz window without exposure to air. The synchronous 2D correlation spectrum in the NIR region illustrated that the melting of ice crystals and the relaxation and proteolysis of proteins occurred earlier than the relaxation of lipids.

10.2.3 IR and Raman Spectra

Vibrational spectroscopic techniques (Raman and IR spectroscopies) have proven to be powerful tools in elucidating protein, lipid, carbohydrate, and water structural characteristics, noninvasively and in situ, in food and particularly in meat, (Herrero 2008a,b; Damez and Clerjon, 2008). Because meat is composed mainly of proteins, lipids, and water, Raman and IR spectral regions of these compounds will be analyzed in the following. Changes in the frequencies, half-widths, and intensities of the Raman and IR bands of chemical groups of these compounds are indicative of structural changes. However, since meat is a complex system comprising mainly proteins, lipids and water, analysis of particular meat components should be carried out after previous removal of any spectral influence from the rest of components (see Section 10.2.2).

10.2.3.1 IR Spectra

NIR spectroscopy provides little interpretable protein and lipids structural information because the broad bandwidth leads to severe overlap of most of the bands in the NIR spectra. As a consequence, NIR has not been used for in-depth study of protein and lipid structural changes in foods and particularly in meat. However, near-IR reflectance spectroscopy (NIRS) in combination with chemometric analysis or other techniques such as imaging techniques (called HSI system) has been used in muscle-based foods such as meat to determine the content of its main constituents (Wold and Isaksson, 1997; González-Pérez et al., 2002, Afseth et al., 2005; Khodabux et al., 2007), to distinguish between storage conditions (Thyholt and Isaksson, 1997; Uddin and Okazaki, 2004) and for assessing food quality (Liu et al.,

2003; McGlone et al., 2005; Ripoll et al., 2008; Prieto et al., 2009; ElMasry et al., 2012 a; Qu et al., 2015). Instead, mid-IR spectroscopy can provide information related to protein secondary structure and carbohydrate, water and lipid structure through well-defined IR characteristics bands. The most characteristic bands appearing in the mid-IR spectra of proteins, lipids and water are described below.

Proteins

IR amide I, amide II, and amide III bands should be mentioned as the main bands providing information related to protein secondary structure. In addition, other bands generated by aliphatic and aromatic amino acid residues provide details on protein tertiary structure. Variations in intensity and/or shifting in frequency of these IR bands evidence protein structural changes (Surewicz and Mantsch, 1984; Barth 2007; Herrero et al., 2010). The amide I vibrational mode is found in the 1700- to 1600-cm^{-1} region (Fig. 10.1), with strong intensity, and is mainly due to the carbonyl stretching vibration with a minor contribution from C−N stretching and N−H bending vibrations. This band mostly depends on the secondary structure of protein backbone. In food with high water content, such as meat products, samples have been previously deuterated to avoid water absorption in the protein spectral region (Herrero et al., 2012). In this way vibrational frequencies are usually shifted to lower values. Proteins adopting α-helical conformation have strong

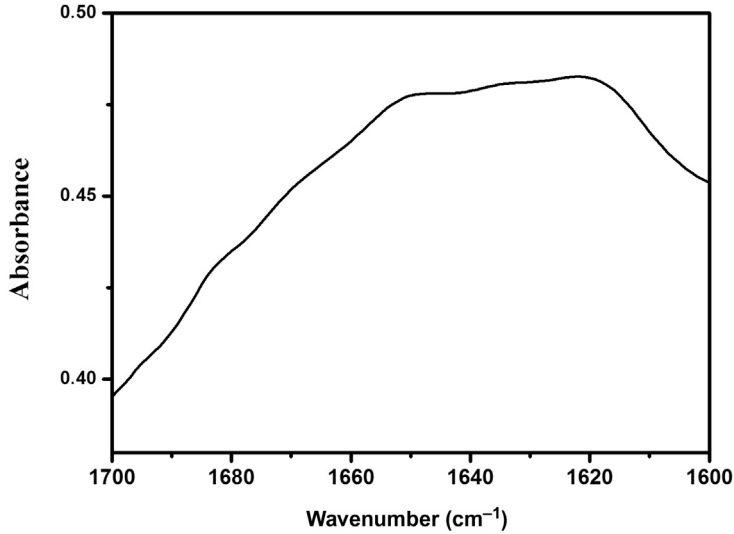

FIGURE 10.1 Typical Fourier transform infrared spectra from a low-fat frankfurter (elaborated with pork meat) in the 1700- to 1600-cm^{-1} region. These spectra were measured from a small portion of deuterated samples using CaF_2 window for transmission infrared spectroscopy.

amide I bands between 1657 and 1650 cm^{-1}, whereas bands between 1640 and 1612 cm^{-1} are commonly associated with β-sheets. The strong water absorption at 1640 cm^{-1} significantly overlaps the amide I band. The amide II band appears in the 1560- to 1510-cm^{-1} range with strong−medium intensity. The other visible amide vibrational mode corresponds to the amide III band which falls in the 1300- to 1200-cm^{-1} region.

Detailed quantitative analysis of amide I and amide II bands is not always an easy task because there is considerable overlapping of a number of bands due to various different secondary structures. The most popular data-processing techniques that avoid overlapping in estimation of protein secondary structures involve either conversion of the spectrum to its second derivative or reduction of the width of the bands by Fourier self-deconvolution of the amide I region to a sum of Lorentzian band components with a nonlinear least-squares procedure (Surewicz and Mantsch, 1984; Herrero et al., 2010, 2012).

Three prominent bands can also be observed in the IR spectra in the 3000- to 2800-cm^{-1} region, which are generated mainly by νCH vibrational modes of amino acids (Surewicz and Mantsch, 1984; Barth, 2007; Herrero et al., 2010).

A strong band at about 3300 cm^{-1} and a somewhat less-strong band at about 3100 cm^{-1} are referred to as the amide A and amide B bands, respectively (Surewicz and Mantsch, 1984; Barth 2007; Herrero et al., 2010). The amide A band is attributed to the νNH vibration, whereas the amide B band is assigned to the first overtone of the amide II vibration, which is intensified by Fermi resonance with the amide A vibration. Changes in these IR bands are associated with changes in secondary structure of proteins.

Lipids

The mid-IR spectra of lipids contain several bands in the 3000- to 1700-cm^{-1} region, and overlapping bans in the 1500- to 700-cm^{-1} region. In these spectra a weak band appears near 3005 cm^{-1} which is generated by the *cis* double-bond CH stretching vibration (νCH =) of lipids. This band is accompanied by methyl group absorption, with characteristic $\nu_s CH_3$ and $\nu_{as} CH_3$ bands appearing as shoulders at approximately 2954 and 2870 cm^{-1}. In addition, the IR region between 3000 and 2500 cm^{-1} is dominated by two strong bands at 2925 and 2854 cm^{-1} (Fig. 10.2) resulting, respectively, from the asymmetric and the symmetric stretching vibrations of the acyl CH_2 groups of lipids (Guillen and Cabo, 1997a,b; van de Voort, Sedman, and Russin, 2001). Modifications of the half-bandwidth of these bands can be generated by changes in lipid chain order/disorder resulting from protein−lipid interactions (Fraile et al., 1999). Narrowing of the spectral profile of these bands (2922 cm^{-1} ($\nu_{as} CH_2$) and 2852 cm^{-1} ($\nu_s CH_2$)) is generally attributed to increasing conformational order of lipid acyl chains (Fraile et al., 1999). In

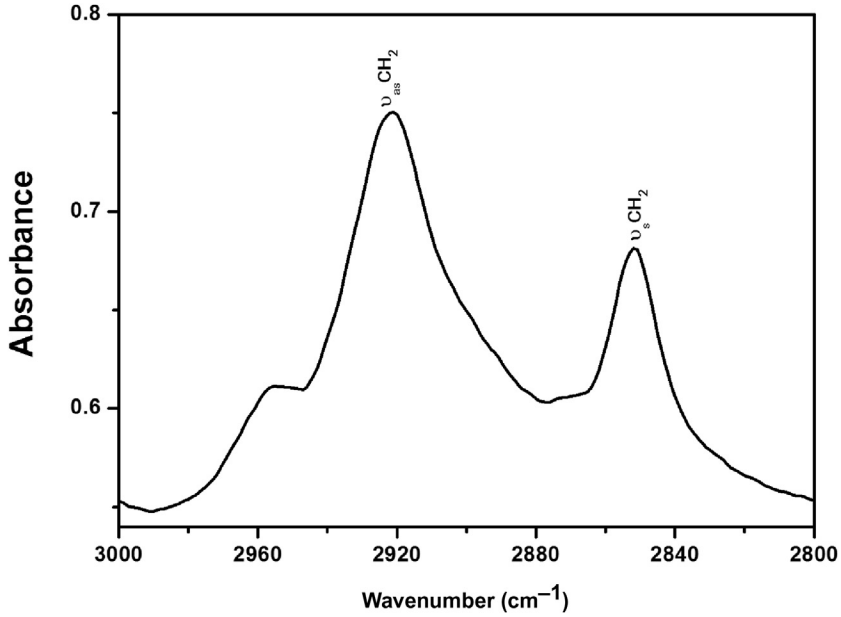

FIGURE 10.2 Fourier transform infrared spectra in the 3000- to 2800-cm^{-1} region from a frankfurter (elaborated with pork meat). These spectra were measured from a small portion of samples using CaF_2 window for transmission infrared spectroscopy and spectral influence of proteins and water should be appropriately substracted.

complex foods such as meat products which contain lipids, protein, and water, any spectral influence of proteins and water should be appropriately subtracted (Herrero et al., 2012) before analyzing lipid structural features in this spectral region.

Additionally, the strong band of the C = O stretching vibration of the carbonyl groups of triglycerides is observed at about 1745 cm^{-1} (Ayora-Cañada et al., 2010). Some bands appearing in the 1400- to 1200-cm^{-1} region can be attributed to bending vibrations of CH_2 and CH_3 aliphatic groups, and the 1125- to 1095-cm^{-1} region includes characteristic bands of C−O the stretching vibration ester groups. Finally, below 1000 cm^{-1}, the band near 723 cm^{-1} is due to the overlapping of the CH_2 rocking vibration and the out-of-plane vibration of *cis*-di-substituted olefins. The major changes occurring in this IR band are due to oxidation (van der Voort et al., 1994). The 723-cm^{-1} band decreases in accordance with the loss of *cis* double bonds due to their isomerization to *trans* groups and/or their breakdown to produce secondary oxidation products. A small absortion increase can generally be observed in the 1400- to 1000-cm^{-1} region. The absorbance increasing in the 1735- to 1660-cm^{-1} region due to oxidation is attributed to carbonyl compounds formed during oxidation. Also, a significant decrease in intensity

is observed for the band located at 3008 cm^{-1}, which derives from the loss in *cis* double bonds (Ayora-Cañada et al., 2010).

Water

A broad absorption band in the 3600- to 3100-cm^{-1} region corresponds to the characteristic O−H stretching vibration and hydrogen bond of the hydroxyl groups. It has been well established that there are two competing structures in the short living molecular order in water: a tetrahedral ice-like arrangement and a nontetrahedral arrangement (McDonald et al., 1986; Marechal, 1991; Kusualik et al., 1994). The component bands of the O−H stretching spectral profile of water in the 3650- to 3000-cm^{-1} region are broadly assigned to two categories. The bands at lower frequencies, approximately 3300- to 3000-cm^{-1}, correspond to the strong hydrogen-bonded patches of molecules with a tetrahedral structure whereas the bands at higher frequencies (3650- to 3300-cm^{-1}) are related to the weak hydrogen-bonded water molecules. Several studies have also shown that water molecule dynamics are significantly disturbed in confined geometries owing to interaction with hydrophilic or hydrophobic substrates at various levels of hydration (Benham et al., 1989; Bergman and Swenson, 2000; Brovchenko et al., 2000; Zanotti et al., 1999).

10.2.3.2 Raman Spectrum

Proteins

Raman spectroscopy provides information on the peptide backbone structure, mainly by means of the amide I and III bands, which are directly related to secondary structure, and the effect of peptide structure on the environment of some side chains such as those of aliphatic, tyrosine, and tryptophan residues, and on the local conformations of disulfide bonds and methionine residues related to tertiary protein structure (Tu, 1982; Tuma, 2005). The characteristic protein Raman bands of interest are described below.

Amide I and III bands: The most useful Raman bands for determining the secondary structure of meat protein (α-helix, β-sheet, turn, unordered) correspond to the amide I and amide III vibrational modes. Fig. 10.3 shows a typical FT-Raman spectrum of a low-fat frankfurter in the 600- to 1800-cm^{-1} region showing both amide I and amide III bands. The contribution of lipids and water molecules in the Raman spectra have to first be appropriately subtracted from the spectra to study protein Raman bands (Alix et al., 1988; Herrero et al., 2008b; Herrero et al., 2014). The strong band centered around 1650- to 1658-cm^{-1} has been assigned unambiguously to the amide I vibrational mode (Krimm and Bandekar, 1986), which involves mainly C = O stretching. Generally speaking, proteins with high α-helical content show an amide I band centered around 1650- to 1658-cm^{-1} (Fig. 10.3), while those with predominantly β-sheet structures show the band between 1665 and 1680 cm^{-1}, and a high proportion of unordered structure is attributable to

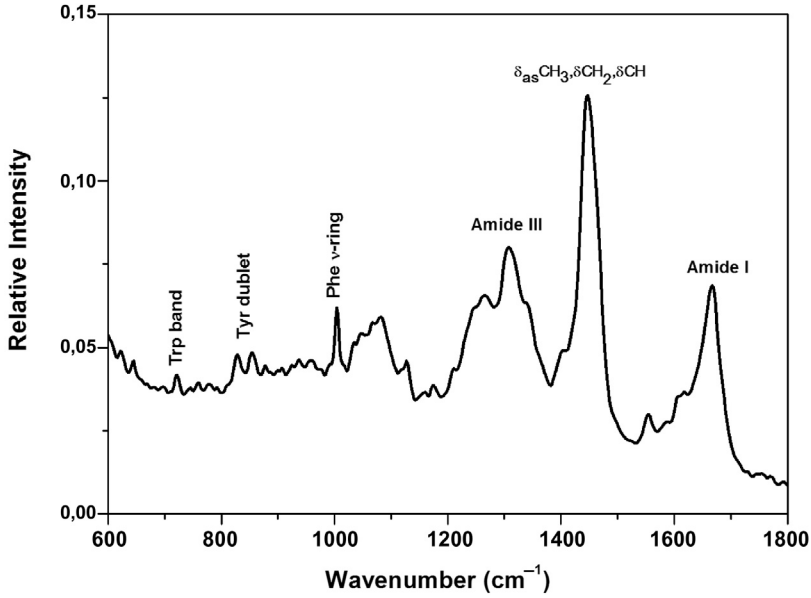

FIGURE 10.3 Typical Fourier transform-Raman spectrum of a low-fat frankfurter (elaborated with pork meat) in the 600- to 1800-cm^{-1} region, where the contribution of lipids and water molecules have been appropriately subtracted from the spectra.

proteins with an amide I band centered at 1660−1665 cm^{-1}. The spectral profile of the amide I band is used to quantify the secondary structure of proteins in terms of α-helix, β-sheet, turn, and unordered (Williams 1983; Alix et al., 1988). However, the contribution of O−H bending vibrations of water molecules in the 1640-cm^{-1} region of Raman spectra has to first be subtracted from the spectra (Alix et al., 1988).

The so-called amide III modes involve C−N stretching and N−H in-plane bending vibrations of the peptide bond as well as contributions from Cα-C stretching and Ci=O in-plane bending. The amide III band is widely used to confirm the results obtained from the amide I band, but is difficult to interpret because proteins produce a complex pattern of bands in the 1225- to 1350-cm^{-1} range (Fig. 10.3) (Krimm and Bandekar, 1986; Pelton and McLean, 2000; Schweitzer-Stenner, 2006).

C−C stretching bands: C−C stretching vibrations in the 890- to 1060-cm^{-1} range are characteristic of α-helix (890−945 cm^{-1}) and β-sheet (1020−1060 cm^{-1}) structures. The gradual loss of these structures has been shown to lead to broadening and weakening in the intensity of this band (Tu, 1982).

Tryptophan residues bands: Tryptophan (Trp) vibrations are visible at 544, 577, 760, 879, 1014, 1340, 1363, 1553, and 1582 cm^{-1} (Thomas, 2002; Combs et al., 2005). A high-intensity ratio of I_{1360}/I_{1340} indicates a

hydrophobic environment, whereas a low-intensity ratio indicates that the Trp residue is involved in the H-bonding of a hydrophilic environment. Modifications in the tertiary structure of proteins can be accompanied by exposure of buried tryptophan residues in proteins, which is observed by a decrease in intensity at 760 cm^{-1} (Tu, 1986) (Fig. 10.3).

Tyrosyl doublet: The ratio of the tyrosyl (Tyr) doublet at 850 and 830 cm^{-1} (Fig. 10.3) is known to be a good indicator of the hydrogen bonding of the phenolic hydroxyl group. The Tyr doublet ratio has been proposed for determining whether the Tyr residue is solvent exposed or buried. When the intensity of the 850-cm^{-1} band is higher than that of the band near 830 cm^{-1} the Tyr residue is exposed, involving changes in the tertiary structure, whereas $I_{850} < I_{830}$ could be interpreted as indicating an increase in the extent to which the tyrosine residues are buried within the protein network (Tu, 1986; Thomas, 2002).

Aliphatic amino acids bands: The bands assigned to the CH_2 scissoring and CH_3 antisymmetric bending vibrations ($\delta_{as}CH_3$, δCH_2, δCH) is observed near 1450 cm^{-1} (Fig. 10.3), and a decrease in the relative intensity of this band may result from hydrophobic interactions of aliphatic residues (Verma and Wallach, 1977).

The bands near 2860, 2935, and 2970 cm^{-1} are assigned to C−H stretching motions ($\nu_s CH_2$ (2860 cm^{-1}), $\nu_{as}CH_2$ (2935 cm^{-1}), and $\nu_{as}CH_3$ (2970 cm^{-1})). It has been shown that exposure of the aliphatic hydrophobic side chains of proteins to an aqueous environment results in increasing intensity of these bands (Verma and Wallach, 1977).

Other bands in the Raman spectra of proteins: A band at 1003−1006 cm^{-1} is attributed to the ν_{12} in-plane ring deformation of the phenylalanine (Phe) ring (Fig. 10.3). The intensity and location of the phenylalanine band is reported to be insensitive to conformation or microenvironment and therefore it may be used as an internal standard (Tu, 1986).

Proteins and peptides with disulfide bonds of cystine show a band centered at 510 cm^{-1} when the C−C−S−S−C−C group is in a "*gauche-gauche-gauche*" conformation. For disulfide bonds in the "*gauche-gauche-trans*" and "*trans-gauche-trans*" conformations, additional bands appear at 525 and 540 cm^{-1}, respectively (Li-Chan et al., 1994). The C−S bonds of methionine and cysteine residues show their stretching vibrations in the 600- to 750-cm^{-1} region, depending on the conformation of the C−S bond. For example, the C−S bond of methionine in the *trans* form shows stretching bands at 655 and 724 cm^{-1}, whereas in the *gauche* form a band appears at around 700 cm^{-1} (Li-Chan et al., 1994). The bands generated by disulfide and C−S bonds in most cases are masked by the librational broad band of water and so often cannot be observed.

A weak Raman band in the 2550- to 2580-cm^{-1} region is attributed to stretching vibration of the S-H group of cysteine residues (Li-Chan et al., 1994).

Aspartic and glutamic acid residues show a Raman band in the 1400- to 1420-cm^{-1} region attributed to the symmetric O−C−O stretching mode of carboxylate groups. The C=O stretch of nonionized COOH groups exhibits a band in the 1700- to 1720-cm^{-1} range. The relative intensity of these bands has been proposed for determining the ionization state of the carboxyl groups (Tu, 1986).

In D_2O solutions of histidine and proteins containing histidine residues, a strong band appears near 1410 cm^{-1}, which can be used to monitor the ionization state of the imidazolium functional group of this amino acid (Tu, 1986).

Proline and its derivative hydroxyproline, which is commonly found in collagen, show strong Raman scattering due to the pyrrolidine ring. Two bands for proline and another for hydroxyproline residues appear at 921 and 855 cm^{-1}, and 880 cm^{-1}, respectively (Herrero, 2008b).

A Raman band at 160 cm^{-1} is attributed to restricted translational motions of water molecules involved in hydrogen bond interactions. The shifting of the band maximum toward lower frequencies has been explained in terms of water molecules binding to biomolecules such as proteins (Colaianni and Nielsen, 1995; Gniadecka et al., 1998).

Lipids

Raman bands observed in the spectral region below 1800 cm^{-1} can be found at about 1750, 1660, 1440, and 1295 cm^{-1}, and are assigned undoubtedly to the C=O stretching modes, C=C stretching modes, CH_2 scissoring modes, and CH_2 twisting modes of lipids, respectively (Li-Chan et al., 1994; Baeten et al., 1996).

Raman spectroscopy can provide a fast quantitative analysis of the unsaturation degree, *cis*/*trans* isomers ratio as well as the amount of double bonds in lipid hydrocarbon chains (Li-Chan et al., 1994; Baeten et al., 1996). The unsaturation degree of lipids has been measured either by means of area ratio of the C=C stretching band located between 1600 and 1700 cm^{-1} and the C=O stretching band falling in the 1790- to 1710-cm^{-1} range, or by means of area ratio of the C=O stretching band and the scissoring band of CH_2 groups (1543−1382 cm^{-1}). The *cis*/*trans* isomers ratio has been quantified also by considering relative intensities of the 1657- and 1667-cm^{-1} bands, respectively. In addition, the total content of *cis* isomer has been measured from the $I_{1265\ cm^{-1}}/I_{1303\ cm^{-1}}$ intensity ratio, whereby results have been obtained which are close to those provided by gas chromatography analysis (Larsson and Rand, 1973). These studies showed also that the changes in the environment of lipid hydrocarbon chains due to different phases resulted in great differences in the C−H stretching region of Raman spectrum.

Although Raman spectroscopy has not been often used for monitoring edible oil oxidation, it has been reported that the major changes during

oxidation comprise intensity decreasing of a broad band at about 1680−1720 cm^{-1} due to the development of carbonyl compounds (Muik et al., 2005). The 1725-cm^{-1} band is assigned to the C=O stretching of saturated aldehydes and that around 1690 cm^{-1} is assigned to the C = O stretching of conjugated unsaturated aldehydes.

The region between 2800 and 3050 cm^{-1} (Fig. 10.4) is characteristic of the symmetric and asymmetric CH stretching vibrations of methyl and methylene groups of lipids, and can be analyzed once the influence of water molecules and proteins in this Raman spectral region has been properly eliminated (Alix et al., 1988; Herrero et al., 2014). In this region, there are various prominent bands: a CH_3 symmetric stretching band near 2897 cm^{-1}, a CH_2 asymmetric stretching band near 2930 cm^{-1} and a CH_2 symmetric stretching motion near 2850 cm^{-1} (Fig. 10.4). Another Raman band can be found at about 3007 cm^{-1} (Fig. 10.4) attributable to *cis*-olefinic group =C-H stretching vibration (Muik et al., 2005; Zou et al., 2009). The symmetric and asymmetric vibrational modes of CH_2 and CH_3 groups can provide insights into interactions between hydrocarbon chains in various states, either in polymorphic forms, emulsions, or in lipid−protein interactions. It has been reported that the peak height intensity ratios $I\nu_sCH_2/I\nu_{as}CH_2$ (I_{2850}/I_{2890}) and $I\nu_sCH_3/I\nu_{as}CH_3$ (I_{2935}/I_{2890}) provide useful indices for gauging lipid packing effects, and determining relative order/disorder of the intermolecular lipid chain (Larsson and Rand, 1973; Larsson, 1976; Carmona et al., 1987; Levin and Lewis, 1990). In particular, the $I\nu_sCH_2/I\nu_{as}CH_2$ index reflects

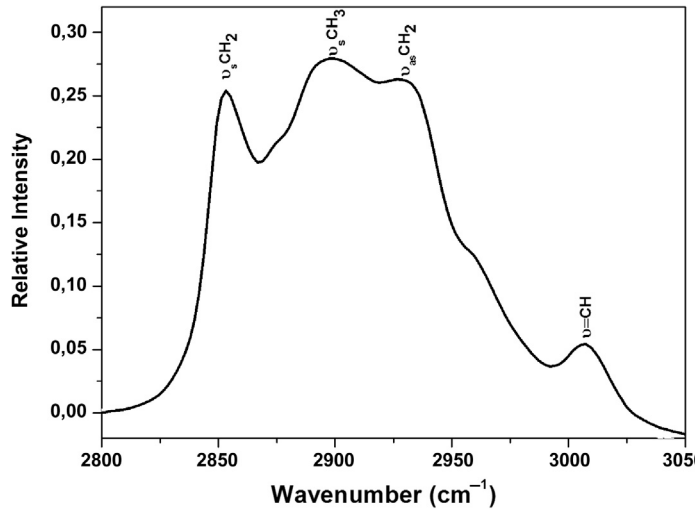

FIGURE 10.4 Raman spectra in the 2800- to 3050-cm^{-1} region from a frankfurter (elaborated with pork meat) where the contributions of lipids and water molecules have been appropriately subtracted from the spectra.

primarily interchain interactions, whereas the $I\nu_{as}CH_2/I\nu_sCH_3$ intensity ratio measures effects originating from changes in intrachain *trans*/*gauche* isomerization superimposed on the chain−chain interactions (Levin and Lewis, 1990).

Water Molecules

The structure of water is reflected in the Raman spectrum through a band appearing near 180 cm^{-1}. This band constitutes direct evidence of hydrogen bonding, and its intensity has been explained as dependent on the concentration of O−H•••O units (Walrafen and Fisher, 1986; Maeda and Kitano, 1995). The band of free water at 180 cm^{-1} shifts toward lower frequencies (120−160 cm^{-1}) when the H_2O molecular species are attached to macromolecules (bound water). This band is attributable to vibrational modes of atoms involved in hydrogen bonding occurring, for instance, in water−protein and protein−protein interactions. The intensity decreasing or absence of the 180-cm^{-1} band is indicative of loss of hydrogen bonds.

The intramolecular vibrations of hydrogen-bonded water molecules comprise two OH stretching bands in the 2800- to 3500-cm^{-1} region and one band of angular deformation appearing around 1645 cm^{-1} (Maeda and Kitano, 1995). This deformation band is characterized by low intensity, and hence is masked by the amide I band located near 1650 cm^{-1}. Some authors have established certain correlations between the microscopic sizes of water domains and the spectral profile of the OH band in the 3000- to 3500-cm^{-1} region (Lafleur et al., 1989).

10.3 APPLICATION OF VIBRATIONAL SPECTROSCOPY FOR MEAT QUALITY ASSESSMENT

Vibrational spectroscopy combined with chemometric analysis has been gaining popularity as a tool to assess meat quality, since there seems to be a significant relationship between structural changes determined through spectral data and sensorial and technological properties results evaluated with methodologies commonly used to determine quality in meat. Chemometric methods in spectroscopic analysis are mathematical or statistical methods used to handle the spectroscopic data. In this context, different multivariate statistic methods are applied to the spectroscopic data to assess meat quality such as: principal component analysis (PCA), partial least-squares regression (PLSR), multiple linear regressions (MLR), classical least-square (CLS), artificial neural network, and many other methods. The advantage of multivariate statistics is that they permit analysis of numerous spectra and spectral regions simultaneously. Additionally, vibrational spectroscopy has considerable advantages that are relevant when searching for a tool for quality assessment, namely high specificity, no need for sample preparation, noninvasive,

need for only a small amount of sample, and it provides information about different compounds at the same time, among others. Another advantage is the fact that over recent years, handheld instruments have been developed that have led to a further extension of the range of applications of vibrational spectroscopy for the quality assessment of food. In particular, Raman and IR portable handheld devices have been developed to predict meat quality and demonstrate their potential (Zamora-Rojas et al., 2012; Roza-Delgado et al., 2014; Scheier et al., 2015; Fowler et al., 2015).

Numerous studies exist related to the potential of vibrational spectroscopy to determine meat composition, particularly fat content and fatty acid composition (Ripoche and Guillard, 2001; Damez and Clerjon, 2013). However, the relevant application of these spectroscopic techniques to asses meat quality should be noted, as compared with conventional methods used with this aim such as sensory analysis, physicochemical and microbiological methods.

10.3.1 Vibrational Spectroscopy and Sensory Analysis

NIR spectroscopy has been utilized as a technique to quickly evaluate some sensorial properties of meat such as appearance (color, marbling, etc.), odor, flavor, juiciness, tenderness, or firmness (Park et al., 1998; Venel et al., 2001; Liu et al., 2003; Andres et al., 2007; Prieto et al., 2009). The potential of visible and near-IR reflectance NIR spectroscopy to predict sensory characteristics related to the eating-quality of lamb meat samples has been evaluated (Andres et al., 2007). Results evidenced that the most important regions of the spectra to estimate the sensory characteristics are those related to the absorbance of intramuscular fat and water in meat samples. However, NIR spectra present often overlapped to yield broad bands that do not provide high-resolution spectroscopic fingerprints of different molecular functional groups, which subsequently limit the accuracy of the sensorial profiling of the meat. Analysis of a meat sample using an mid-infrared (MIR) spectrum ($4000-400\ cm^{-1}$) probably gives more accurate data. In this context, the potentials of both NIR and FT-IR spectroscopy have been evaluated to investigate meat aging and salting with different types of salt in order to relate spectral results directly to water-binding properties and sensorial attributes (Perisic et al., 2013). HSI techniques based on NIR have received much attention for prediction of the tenderness of meat (Cluff et al., 2008; Naganathan et al., 2008; ElMasry et al., 2012b). Kamruzzaman et al. (2013a,b) developed and tested a HSI system (900−1700 nm) to predict sensory tenderness of lamb meat obtaining partial least squares regression (PLSR) models with reasonable accuracy. The feasibility of predicting sensory characteristics of chicken breasts deboned at 2, 4, 6, and 24 h postmortem by visible/NIRS in the 400- to 1850-nm region was also determined (Liu et al., 2004).

Raman spectroscopy is an alternative to IR spectroscopy to predict some sensorial attributes of meat and meat products (Brøndum et al., 2000; Beattie

et al., 2004; Wang et al., 2012). In these respect, Raman spectra data have been correlated with sensory attributes (juiciness and texture) using PLSR from cooked beef samples (Beattie et al., 2004). A strong positive correlation between protein characteristics Raman bands (amide I band, C−C stretching bands, and aliphatic amino acids bands) and juiciness determined by sensory analysis were found. These results could be related to changes in secondary structure, in terms of increase of β-sheets and decrease of α-helices, as wells as to hydrophobic interactions of aliphatic residues that can be associated to juiciness. Raman data also showed good correlation between with amide I and amide III bands (characteristics of proteins) and textural sensory attributes such as toughness. This fact has been attributed to the increase in β-sheets content in the tough meat. Other Raman bands assigned to protein such as tryptophan residues bands and tyrosyl doublet were related to tough meat samples (Beattie et al., 2004). Some authors reported that some sensory attributes of pork loins are moderately correlated to Raman spectroscopic data in the 400- to 2000-cm^{-1} region (Wang et al., 2012). They developed PLSR models to predict the value of sensory tenderness, chewiness, and juiciness based on Raman spectroscopic data of pork loins. Furthermore, these authors created binary barcodes models based on spectroscopic data to classify pork loins into sensory quality grades ("good" and "bad" in terms of tenderness and chewiness).

10.3.2 Vibrational Spectroscopy and Physicochemical Methods

IR and Raman spectroscopy have been compared to different traditional physicochemical methods (water-holding capacity (WHC), instrumental textural methods, etc.) to asses meat quality treated under different conditions of handling, processing, and storage, mainly through the changes in proteins, water, and lipids in the spectra.

The WHC of meat, defined as the ability to hold its own and/or added water, is one of the most important technological properties of meat because it affects the quality of the end product and can influence consumer preferences (Honikel and Hamm, 1994). Water loss is undesirable in meat due to its influence on the appearance, juiciness, and cooking yield, etc. IR spectroscopy and mainly NIR have been used to evaluate the WHC of meat and meat products such as broiler breast fillets (Hoving-Bolink et al., 2005; Prieto et al., 2009; Samuel et al., 2011; Bowker et al., 2014). The results have shown that there is much controversy in relation to the possibilities of NIR as a potential technique to predict WHC in meat, although some authors reported moderate predictions for this technological property (Prieto et al., 2009; Ripoll et al., 2008; Forrest et al., 2000; Bowker et al., 2014; Barbin et al., 2015). NIR revealed WHC associations with protein, intramuscular fat, and water. Some authors indicated that the most important wavelengths identified for build prediction models of WHC in chicken were 440, 558,

1656, and 1908 nm (Barbin et al., 2015). Linear discriminate analyses were used to classify fillets as high- or low-WHC according to predicted meat quality characteristics. Fillets could be correctly classified into high- and low-WHC groups using the visible spectra (400−750 nm) with 88%−92% accuracy and using the NIR spectra (750−2500 nm) with 74%−76% accuracy (Bowker et al., 2014). Additionally, a HSI technique in VIS/NIR region was tested to investigate the ability of the technique for determining WHC in red meat accompanied with multivariate analysis by identifying dominant feature wavelengths related to WHC (ElMasry, Sun and Allen, 2011; Kamruzzaman et al., 2016a). Studies in fresh pork meat revealed a high correlation between WHC and FT-IR spectra using PLSR. Pedersen et al. (2003) indicated that the IR region 1800−900 cm^{-1} contains the best predictive information which covers the functional group frequencies of water, protein, fat, and glycogen, including the carbonyl and amide groups. This research included the possibilities of Raman spectroscopy to determine WHC and showed that Raman spectral regions of interest to WHC according to PLSR results are related to protein conformation (Pedersen et al., 2003). In particular, WHC has been related to changes in Raman region containing NH stretching bands of amide groups in proteins (3071–3128 cm^{-1}) and C−C stretching bands (876−951 cm^{-1}) which indicated modifications in secondary structure of proteins (α-helix structure) (Pedersen et al., 2003). Raman spectroscopy also provided good predictive information for WHC of chicken breast meat using specific bands (538, 691, 1367, 1743 cm^{-1}) and amide I and III regions (Phongpa-Ngan et al., 2014).

Other technological properties which define in many cases the quality of muscle-based foods, since they determine to a great extent the product acceptance by consumers, are textural characteristics. Textural characteristics are associated with the intrinsic structure and properties of components of the muscle. Myofibrillar proteins, among the meat muscle components, are the main contributors imparting textural attributes. There are several instrumental methods to determine textural properties of meat, among them texture profile analysis (TPA), the Kramer shear-compression cell method, the puncture test, the Warner−Bratzler cell method, etc. (Bourne, 2002). In this context, Kamruzzaman et al. (2013a,b) developed and tested a HSI system (900−1700 nm) to predict instrumental tenderness of lamb meat. The Warner−Bratzler cell method was performed and shear force (WBSF) values were used as instrumental texture parameters. They obtained PLSR models with reasonable accuracy. The results confirmed that the spectral data could become an interesting screening tool to quickly categorize lamb steaks into good (i.e., tender) and bad (i.e., tough) based on WBSF values and sensory scores (Kamruzzaman et al., 2013a,b). Since WBSF is an important index of meat tenderness the possibilities of Fourier transform near-IR (FT-NIR) were also evaluated to determine this texture parameter as well as others (Andrés et al., 2008; Bowling et al.,

2009; Cai et al., 2011). Some authors performed a synergy interval partial least square (SI-PLS) algorithm to calibrate a regression model for WBSF. Experimental results showed that the correlations coefficients in the calibration set (R_c) and prediction set (R_p) were 0.7533 and 0.7041, respectively, for the WBSF model. The overall results demonstrated that NIR spectroscopy combined with SI-PLS could be utilized to determine WBSF in pork (Cai et al., 2011). The feasibility of predicting shear force of chicken breasts deboned at 2, 4, 6, and 24 h postmortem by visible/NIRS in the 400- to 1850-nm region was determined (Liu et al., 2004). On the basis of predicted shear values from the partial least-squares (PLS) model, breast samples were classified into "tender" or "tough" classes with a correct classification of 74.0%. FT-IR and FT-Raman spectroscopy were useful to relate textural behavior and structural characteristics in meat and meat products (Herrero et al., 2008c; Xu et al., 2011; Carmona et al., 2011; Herrero et al., 2012, 2014). These spectroscopic techniques have been used to evidence structural changes in meat components during processing and storage that have been correlated with textural properties of the product. In particular, these techniques have been used to study the relationship between texture of meat products and conformational modifications in meat components induced by storage and processing such as different salt concentrations, heating, or the incorporation of nonmeat ingredients (soy protein, kappa-carrageenan, wheat dietary fiber, cold gelling agents, olive oil bulking agents, etc.), in most cases with the aim of developing healthy foods (Chattong et al., 2007; Herrero et al., 2008c, d, 2012, 2014; Carmona et al., 2011; Shao et al., 2011; 2015; Gao et al., 2015). In general the incorporation of these ingredients produced frequency upshifting and profile modifications of amide I attributed to an increase of β-sheet structure. In most studies, structural changes in proteins and lipids have been seen to be correlated with specific textural characteristics of meat products (Shao et al., 2011; Herrero et al., 2014, Gao et al., 2015).

Both IR and Raman spectroscopy have also been used to predict other meat physicochemical quality attributes commonly used as a quality index for the meat industry and meat science research such as color, pH, markers of deterioration, etc. (Prieto et al., 2009; Cai et al., 2011; Barbin et al., 2015; Fowler et al., 2015). However, since some cases such as studies evaluating NIR spectroscopy to predict pH or color (in terms of lightness (L^*), redness (a^*) and yellowness (b^*) parameters) the results obtained are contradictory (Prieto et al., 2009), a NIR HSI system has been also used for predicting pH and L* values in beef, lamb, and pork (ElMasry et al., 2012b; Kamruzzaman et al., 2012; Barbin et al., 2012). Recently, a visible NIR HSI system in the spectral range of 400−1000 nm was tested to develop an online monitoring system for red meat (beef, lamb, and pork) color (L^*, a^*, b) in the meat industry (Kamruzzaman et al., 2016b). Only

six wavelengths (450, 460, 600, 620, 820, and 980 nm) were further chosen as predictive feature wavelengths for predicting L^*, a^*, and b^* in red meat. Multiple linear regression models were then developed and predicted L^*, a^*, and b^* with coefficients of determination (R) of 0.97, 0.84, and 0.82, respectively. The results indicated that HSI has the potential to be used for rapid assessment of meat color. Some studies were conducted to determine the potential for a Raman spectroscopic handheld device to predict meat quality traits of fresh lamb (Fowler et al., 2015; Scheier et al., 2015). Results indicated a potential to predict pH and L^* values among other parameters.

10.3.3 Vibrational Spectroscopy and Microbiological Analysis

Microbial spoilage plays a very important role in food safety and quality evaluation. The degree of microbiological spoilage which the meat has undergone affects product safety and quality. Muscle food is one of the most perishable food products because of its vulnerability to microbial spoilage, which can result in critical food safety problems. Traditional techniques for detection and evaluation of microbial spoilage in muscle foods have several drawbacks. They are tedious, laborious, destructive, and time-consuming. Some rapid microbiological methods have been developed during the last decade and some of these automated procedures could be used. However, in the majority of rapid methods, large numbers of samples are needed. Therefore, it is recommended that novel techniques be developed that limited these drawbacks. In this respect, vibrational spectroscopic techniques could be a promising alternative. Recently, several studies have shown that the HSI system in the visible and near-IR range (400−1100 nm), in combination with other classical microbiological methods and chemometric analysis as PLSR models, was able to detect the bacterial spoilage in chicken meat (Feng and Sun, 2012; Xiong et al., 2015; Cheng and Sun, 2015). Results demonstrated the feasibility of using this spectroscopic technique as a valid means for nondestructive determination of total viable counts (TVC) in chicken fillet samples, as well as detecting specific bacteria such as *Enterobacteriaceae* and *Pseudomonas* using selected wavelengths (Feng and Sun, 2013; Feng et al., 2013). Some authors have also evaluated the possibilities of FT-IR to be used for the rapid assessment of meat spoilage (TVC, *Pseudomonas* spp., lactic acid bacteria (LAB), *Enterobacteriaceae*, etc.) (Ellis et al., 2002; 2004; Ammor et al., 2009; Papadopoulou et al., 2011; Argyri et al., 2013; Cheng and Sun 2015). FT-IR was used directly from the sample surface using ATR, while in parallel the TVC of bacteria were obtained by traditional microbiological methods (Ellis et al., 2004; Ammor et al., 2009). Quantitative interpretation of FT-IR spectra was undertaken using PLSR and allowed for accurate estimates of bacterial loads to be calculated directly from the meat surface in 60 s (Ellis et al., 2004).

Machine-learning methods in the form of genetic algorithms and genetic programing were used to elucidate the wavenumbers of interest related to the spoilage process. The results obtained demonstrated that, using FT-IR and machine learning, it was possible to detect bacterial spoilage rapidly in beef and that the most significant functional groups selected could be directly correlated to the spoilage process which arose from proteolysis, resulting in changes in the levels of amides and amines (Ellis et al., 2004). FT-IR spectra of poultry meat containing specific bacteria (*Salmonella enteritidis*, *Pseudomonas ludensis*, *Listeria monocytogenes* and *Esherichia coli*) were collected and investigated for their classification and quantification (Grewal et al., 2015). Multivariate data analysis techniques PCA, PLS discriminant analysis (PLSDA) and soft independent modeling of class analogy (SIMCA) were used and the highest correct classification results for SIMCA and PLSDA were achieved in the 1200- to 1800-cm^{-1} spectral region. Thus it is seen that FTIR spectroscopy in combination with chemometrics is a powerful technique that can be further developed to differentiate between bacteria on poultry meat surface (Grewal et al., 2015).

Raman spectroscopy coupled with chemometric models is gaining increasing attention for rapid and precise detection of microorganisms (Lu et al., 2011; Cheng and Sun, 2015; He and Sun, 2015). In particular in meat, a combination of Raman microspectroscopy and multivariate analysis (cluster analysis, support vector machine, etc.) was applied to detect pathogens in meat (Meisel et al., 2014). *L. monocytogenes, Salmonella spp.,* ***Staphylococcus*** *aureus and* ***Yersinia*** *enterocolitica* were identified after isolation from artificially contaminated minced beef or chicken breast by a three-level classification model based on support vector machines. Models predictive of the microbiological load were calculated using chemometric analysis (PLSR, genetic programing (GP), genetic algorithm (GA), artificial neural networks, etc.) and Raman spectra data from minced beef samples stored under different packaging conditions (aerobic and modified atmosphere packaging) at 5°C (Argyri et al., 2013). In general, it was observed that for calibration models, better predictions were obtained for TVC, LAB and *Enterobacteriaceae*. The bands that were mostly used were from 2096 to 2140 cm^{-1} and from 3296 to 3400 cm^{-1} for all cases.

In addition, HSI systems have shown their potential for inspecting fecal contaminants in real-time mode during poultry and broiler processing (Windham et al., 2005; Park et al., 2011). The line-scan imaging system utilized an electron-multiplying charge-coupled device (EMCCD) camera and an imaging spectrograph (400−1000, Hyperspect-VNIR) attached to the EMCCD camera (Park et al., 2011). The authors concluded that more research should be carried out to fully validate the performance of this system to detect fecal contaminants for high detection accuracy with minimum false-positive errors.

10.3.4 Vibrational Spectroscopy and Authentication

Meat authenticity is an emerging area of concern for consumers, retailers, and food regulatory bodies, as it guarantees that food has not been subjected to adulteration by any lower-grade material, either by accident of for economic gain. Moreover, meat adulteration can cause some religious problems as, in some countries, with the consumption of certain proscribed meats (e.g., pork). In this concern, vibrational spectroscopic methods are emerging as potential tools for the detection of meat adulteration (Al-Jowder et al., 1999; Reid, O'Donnell and Downey, 2006; Herrero, 2008a; Kamruzzaman et al., 2013a,b; Qu et al., 2015). NIR spectroscopy has been shown to be a potential tool for discrimination of beef from other types of meat, as well as differentiation between different types of beef meat involving various breeds, muscle types, and ages as well (Qu et al., 2015). Preliminary studies has been performed to develop and optimize a rapid analytical technique based on NIR HSI to detect the level of adulteration in minced lamb (Kamruzzaman et al., 2013a,b). Initial investigations were carried out using PCA to identify the most potential adulterate in minced lamb (such as minced pork) and the PLSR model to predict their level of adulteration. The results demonstrated that the laborious and time-consuming tradition of analytical techniques could be replaced by spectral data in order to provide a rapid, low-cost, and nondestructive testing technique for adulterate detection in minced lamb meat (Kamruzzaman et al., 2013a,b). Additionally, it has been reported that mid-IR spectroscopy with attenuated total reflectance (FT-IR-ATR) in conjunction with appropriate chemometrics methods have the potential to be established as a technique for meat authentication (Al-Jowder et al., 1997; 1999; 2002). FT-IR-ATR, PCA, and PLSR have shown their possibilities to distinguish minced chicken, pork and turkey meat from their IR spectra (Al-Jowder et al., 1997). This spectroscopic technique can also discriminate between beef muscle and offal tissue types using PLSR and canonical variate analysis (Al-Jowder et al., 1999).

Some investigations have been performed in meat to evaluate the possibilities of Raman spectroscopy for authentication of meat by substitution of traditional techniques such as detection of DNA or RNA, immunological, electrophoretic, and chromatographic techniques which are destructive and time consuming. In this respect, Raman spectroscopy has been used to discriminate between main meat-type poultry species (turkey and chicken) and anatomical muscle origin (breast and leg) (Ellis et al., 2005). Cluster analysis using Raman spectra in the 0- to 3000-cm^{-1} range showed that the major discrimination ability was between leg and breast meat (Ellis et al., 2005). Other studies have focused on beef offal (i.e., kidney, liver, heart, and lung) adulteration of beef burgers using dispersive Raman spectroscopy and multivariate data analysis to explore the potential of these analytical tools for detection of adulterations in comminuted meat products with complex formulations (Zhao

et al., 2015). Raman spectral data in the fingerprint range (900−1800 cm^{-1}) were examined using both a classification (PLS-DA) and class-modeling (SIMCA) approach to identify offal-adulterated and authentic beef burgers. PLS-DA models correctly classified 89%−100% of authentic and 90%−100% of adulterated samples. Additionally, a novel fat-based method was developed which uses Raman spectroscopy in combination with PCA for the rapid determination of beef adulteration with horsemeat (Boyaci et al., 2014a, b). In order to distinguish pure horse and beef samples from each other, PCA was performed on the entire spectrum between 200 and 2000 cm^{-1} and results showed that the presence of different concentrations (25, 50, and 75%, w/w) of horsemeat in beef was differentiated (Boyaci et al., 2014a).

10.4 CONCLUSIONS

The combination of methods based on vibrational spectroscopy (IR and Raman spectroscopy) with multivariate statistical techniques (chemometrics) has considerable potential and a growing range of uses in the food field, particularly in applications for meat quality assessment. IR spectroscopy has been, and will continue to be, an important analytical tool for this purpose. Even though IR analyzers have already taken part in the process development, scale-up and on the floor of production facilities, the evolution of the technology will continue to bring newer IR instruments that are more flexible, rugged, robust, and easier to implement and operate. Raman spectroscopy is also being used in this area since rich spectral information, sharp well-resolved spectral bands, relative ease of sampling, and process interfacing, provide advantages over many traditional analysis tools. Raman spectroscopy can often reliably predict qualitative and quantitative aspects of meat components and, as Raman technology continues to develop, a wider range of tools and applications in this field will become available. Additionally both IR and Raman spectroscopy show some advantages when compared with traditionally used methodology, since this technique involves analytical direct methods (noninvasive), needs few sample milligrams, and provides information about different meat components at the same time in a unique spectra.

ACKNOWLEDGMENTS

The authors wish to thank MINECO, CAM, and CSIC for financial support of this research, via Projects MEDGAN-CM S2013/ABI2913; AGL2014-53207-C2-1-R, 2014470E073; and 201470E056.

REFERENCES

Afseth, N.K., Segtnan, V.H., Marquardt, B.J., Wold, J.P., 2005. Raman and near-infrared spectroscopy for quantification of fat composition in a complex food model system. Appl. Spectrosc. 59 (11), 1324−1332.

Alix, A.J.P., Pedanou, G., Berjot, M., 1988. Fast determination of the quantitative secondary structure of proteins by using some parameters of the Raman amide I band. J. Mol. Struct. 174, 159–164.

Al-Jowder, O., Kemsley, E.K., Wilson, R.H., 1997. Mid-infrared spectroscopy and authenticity problems in selected meats: a feasibility study. Food Chem. 59 (2), 195–201.

Al-Jowder, O., Defernez, M., Kemsley, E.K., Wilson, R.H., 1999. Mid-infrared spectroscopy and chemometrics for the authentication of meat products. J. Agric. Food Chem. 47 (8), 3210–3218.

Al-Jowder, O., Kemsley, E.K., Wilson, R.H., 2002. Detection of adulteration in cooked meat products by mid-infrared spectroscopy. J. Agric. Food Chem. 50 (6), 1325–1329.

Ammor, M., Argyri, A., Nychas, G.J., 2009. Rapid monitoring of the spoilage of minced beef stored under conventionally and active packaging conditions using Fourier transform infrared spectroscopy in tandem with chemometrics. Meat Sci. 81 (3), 507–515.

Andres, S., Murray, I., Navajas, E.A., Fisher, A.V., Lambe, N.R., Bünger, L., 2007. Prediction of sensory characteristics of lamb meat samples by near infrared reflectance spectroscopy. Meat Sci. 76 (3), 509–516.

Andrés, S., Silva, A., Soares-Pereira, A.L., Martins, C., Bruno-Soares, A.M., Murray, I., 2008. The use of visible and near infrared reflectance spectroscopy to predict beef *M. longissimus thoracis* et *lumborum* quality attributes. Meat Sci. 78 (3), 217–224.

Argyri, A.A., Jarvis, R.M., Wedge, D., Xu, Y., Panagou, E.Z., Goodacre, R., et al., 2013. A comparison of Raman and FT-IR spectroscopy for the prediction of meat spoilage. Food Control 29 (2), 461–470.

Ayora-Cañada, M.J., Domínguez-Vidal, A., Lendl, B., 2010. Monitoring oxidation of lipids in edible oils and complex Food Systems by vibrational spectroscopy. In: Chalmers, J., Griffiths, P., Li-Chan, E. (Eds.), Applications of Vibrational Spectroscopy to Food Science. John Wiley & Sons, New York, pp. 277–296.

Baeten, V., Meurens, M., Morales, M.T., Aparicio, R., 1996. Detection of virgin olive oil by Fourier transform Raman spectroscopy. J. Agric. Food Chem. 44 (8), 2225–2230.

Barbin, D., ElMasry, G., Sun, D.W., Allen, P., 2012. Predicting quality and sensory attributes of pork using near-infrared hyperspectral imaging. Anal. Chim. Acta 719, 30–42.

Barbin, D.F., Kaminishikawahara, C.M., Soares, A.L., Mizubuti, I.Y., Grespan, M., Shimokomaki, M., et al., 2015. Prediction of chicken quality attributes by near infrared spectroscopy. Food Chem. 168, 554–560.

Barth, A., 2007. Infrared spectroscopy of proteins. Biochem. Biophys. Acta 1767 (9), 1073–1101.

Beattie, R.J., Bell, S.J., Farmer, L.J., Moss, B.W., Patterson, D., 2004. Preliminary investigation of the application of Raman spectroscopy to the prediction of the sensory quality of beef silverside. Meat Sci. 66 (4), 903–913.

Benham, M.J., Cook, J.C., Li, J.C., Ross, D.K., Hall, P.L., Sarkissian, B., 1989. Small-angle neutron-scattering study of adsorbed water in porous vycor glass–supercooling phase-transition and interfacial structure. Phys. Rev. B 39, 633–636.

Bergman, R., Swenson, J., 2000. Dynamics of supercooled water in confined geometry. Nature 403, 283–286.

Bourne, M.C., 2002. Principles of objective texture measurement. In: Bourne, M.C. (Ed.), Food Texture and Viscosity: Concept and Measurement. Elsevier Inc, San Diego, CA, pp. 107–188.

Bowker, B., Hawkins, S., Zhuang, H., 2014. Measurement of water-holding capacity in raw and freeze-dried broiler breast meat with visible and near-infrared spectroscopy. Poult. Sci. 93 (7), 1834–1841.

Bowling, M.B., Vote, D.J., Belk, K.E., Scanga, J.A., Tatum, J.D., Smith, G.C., 2009. Using reflectance spectroscopy to predict beef tenderness. Meat Sci. 82 (1), 1–5.

Boyaci, I.H., Temiz, H.T., Uysal, R.S., Velioglu, H.M., Yadegari, R.J., Rishkan, M.M., 2014a. A novel method for discrimination of beef and horsemeat using Raman spectroscopy. Food Chem. 148, 37–41.

Boyaci, I.H., Uysal, R.S., Temiz, T., Shendi, E.G., Yadegari, R.J., Rishkan, M.M., et al., 2014b. A rapid method for determination of the origin of meat and meat products based on the extracted fat spectra by using of Raman spectroscopy and chemometric method. Eur. Food Res. Technol. 238 (5), 845–852.

Brovchenko, I., Paschek, D., Geiger, A., 2000. Gibbs ensemble simulation of water in spherical cavities. J. Chem. Phys. 113, 5026–5036.

Brøndum, J., Byrne, D.V., Bak, L.S., Bertelsen, G., Engelsen, S.B., 2000. Warmed-over flavour in porcine meat-a combined spectroscopic, sensory and chemometric study. Meat Sci. 54 (1), 83–95.

Cai, J., Chen, Q., Wan, X., Zhao, J., 2011. Determination of total volatile basic nitrogen (TVB-N) content and Warner–Bratzler shear force (WBSF) in pork using Fourier transform near infrared (FT-NIR) spectroscopy. Food Chem. 126 (3), 1354–1360.

Carmona, P., Ramos, J.M., de Cózar, M., Monreal, J., 1987. Conformational features of lipids and proteins in myelin membranes using Raman and infrared spectroscopy. J. Raman Spectrosc. 18 (7), 473–476.

Carmona, P., Ruiz-Capillas, C., Jimenez-Colmenero, F., Pintado, T., Herrero, A.M., 2011. Infrared study of structural characteristics of frankfurters formulated with olive oil-in-water emulsions stabilized with casein as pork backfat replacer. J. Agric. Food Chem. 59, 12998–13003.

Chalmers, J.M., Griffiths, P.R., 2007. Sampling techniques and fiber-optic probes. In: Pivonka, E., Chalmers, J.M., Griffiths, P.R. (Eds.), Applications of Vibrational Spectroscopy in Pharmaceutical Research and Development. Wiley, New York, pp. 19–49.

Chattong, U., Apichartsrangkoon, A., Bell, A.E., 2007. Effects of hydrocolloid addition and high pressure processing on the rheological properties and microstructure of a commercial ostrich meat product "Yor" (Thai sausage). Meat Sci. 76 (3), 548–554.

Cheng, J.H., Sun, D.W., 2015. Recent applications of spectroscopic and hyperspectral imaging techniques with chemometric analysis for rapid inspection of microbial spoilage in muscle foods. Comprehen. Rev. Food Sci. Food Saf. 14 (4), 478–490.

Cluff, K., Naganathan, G.K., Subbiah, J., Lu, R., Calkins, C.R., Samal, A., 2008. Optical scattering in beef steak to predict tenderness using hyperspectral imaging in the VIS-NIR region. Sens. Instrum. Food Qual. Saf. 2 (3), 189–196.

Colaianni, S.E.M., Nielsen, O.F., 1995. Low-frequency Raman spectroscopy. J. Mol. Struct. 347, 267–284.

Combs, A., McCann, K., Autrey, D., Laane, J., Overman, S.A., Thomas Jr, G.J., 2005. Raman signature of the non-hydrogen-bonded tryptophan side chain in proteins: experimental and ab initio spectra of 3-methylindole in the gas phase. J. Mol. Struct. 735–736, 271–278.

Cozzolino, D., 2015. The role of vibrational spectroscopy as a tool to assess economically motivated fraud and counterfeit issues in agricultural products and foods. Anal. Methods 7 (22), 9390–9400.

Damez, J.L., Clerjon, S., 2008. Meat quality assessment using biophysical methods related to meat structure. Meat Sci. 80 (1), 132–149.

Damez, J.L., Clerjon, S., 2013. Quantifying and predicting meat and meat products quality attributes using electromagnetic waves: an overview. Meat Sci. 95 (4), 879–896.

Ellis, D.I., Broadhurst, D.I., Goodacre, R., 2004. Rapid and quantitative detection of the microbial spoilage of beef by Fourier transform infrared spectroscopy and machine learning. Anal. Chim. Acta 514, 193–201.

Ellis, D.I., Broadhurst, D., Clarke, S.J., 2005. Rapid identification of closely related muscle foods by vibrational spectroscopy and machine learning. Analyst 130, 1648–1654.

Ellis, D.I., Broadhurst, D., Kell, D.B., Rowland, J.J., Goodacre, R., 2002. Rapid and quantitative detection of the microbial spoilage of meat by Fourier transform infrared spectroscopy and machine learning. Appl. Environ. Microbiol. 68 (2), 2822–2828.

ElMasry, G., Sun, D.W., Allen, P., 2011. Non-destructive determination of water holding capacity in fresh beef by using NIR hyperspectral imaging. Food Res. Int. 44 (9), 2624–2633.

ElMasry, G., Barbin, D.F., Sun, D.W., Allen, P., 2012a. Meat quality evaluation by hyperspectral imaging technique: an overview. Crit. Rev. Food Sci. Nutr. 52 (8), 689–711.

ElMasry, G., Sun, D.W., Allen, P., 2012b. Near-infrared hyperspectral imaging for predicting colour, pH and tenderness of fresh beef. J. Food Eng. 44 (1), 2624–2633.

FAO (Food and Agriculture Organization), 2012. World agriculture towards 2030/2050: the 2012 revision. In: Alexandrato, N., Bruinsma, J., (Eds.) ESA Working Paper No. 12-03. Available from: http://www.fao.org/docrep/016/ap106e/ap106e.pdf. (13 December 2016).

Feng, Y.Z., Sun, D.W., 2012. Application of hyperspectral imaging in food safety inspection and control: a review. Crit. Rev. Food Sci. Nutr. 52 (11), 1039–1058.

Feng, Y.Z., Sun, D.W., 2013. Determination of total viable count (TVC) in chicken breast fillets by near-infrared hyperspectral imaging and spectroscopic transforms. Talanta 105, 244–249.

Feng, Y.Z., ElMasry, G., Sun, D.W., Scannell, A.G., Walsh, D., Morcy, N., 2013. Near-infrared hyperspectral imaging and partial least squares regression for rapid and reagentless determination of *Enterobacteriaceae* on chicken fillets. Food Chem. 138 (2–3), 1829–1836.

Forrest, J.C., Morgan, M.T., Borggaard, C., Rasmussen, A.J., Jespersen, B.L., Andersen, J.R., 2000. Development of technology for the early post mortem prediction of water holding capacity and drip loss in fresh pork. Meat Sci. 55 (1), 115–122.

Fowler, S.M., Schmidt, H., van de Ven, R., Wynn, P., Hopkins, D.L., 2015. Predicting meat quality traits of ovine m. semimembranosus, both fresh and following freezing and thawing, using a hand held Raman spectroscopic device. Meat Sci. 118, 138–144.

Fraile, M.V., Patrón-Gallardo, B., López-Rodríguez, G., Carmona, P., 1999. FT-IR study of multilamellar lipid dispersions containing cholesteryl linoleate and dipalmitoylphosphatidylcholine. Chem. Phys. Lipids 97 (2), 119–128.

Gao, X.Q., Kang, Z.L., Zhang, W.G., Li, Y.P., Zhou, G.H., 2015. Combination of kappa-carrageenan and soy protein isolate effects on functional properties of chopped low-fat pork batters during heat-induced gelation. Food Bioprocess Technol. 8 (7), 1524–1531.

Gniadecka, M., Nielsen, O.F., Christensen, D.H., Wulf, H.C., 1998. Structure of water, proteins and lipids in intact human skin, hair and nail. J. Investig. Dermol. 110 (4), 393–398.

González-Pérez, C., Hernández-Méndez, J., Álvarez-García, N., Andaluz, J.L.H., 2002. On-line non-destructive determination of proteins and infiltrated fat in Iberian pork loin by near infrared spectrometry with a remote reflectance fibre optic probe. Anal. Chim. Acta 453 (2), 281–288.

Grewal, M.K., Jaiswal, P., Jha, S.N., 2015. Detection of poultry meat specific bacteria using FTIR spectroscopy and chemometrics. J. Food Sci. Technology-Mysore 52 (6), 3859–3869.

Guillen, M.D., Cabo, N., 1997a. Characterization of edible oils and lard by Fourier transform infrared spectroscopy. Relationships between composition and frequency of concrete bands in the fingerprint region. J. Am. Oil Chem. Soc. 74 (10), 1281–1286.

Guillen, M.D., Cabo, N., 1997b. Infrared spectroscopy in the study of edible oils and fats. J. Sci. Food Agric. 75 (1), 1–11.

He, H.J., Sun, D.W., 2015. Microbial evaluation of raw and processed food products by Visible/Infrared, Raman and Fluorescence spectroscopy. Trends Food Sci. Technol. 46 (2), 199–210.

Herrero, A.M., 2008a. Raman spectroscopy a promising technique for quality assessment of meat and fish: a review. Food Chem. 107 (4), 1642–1651.

Herrero, A.M., 2008b. Raman spectroscopy for monitoring protein structure in muscle food systems. Crit. Rev. Food Sci. Nutr. 48 (6), 512–523.

Herrero, A.M., Carmona, P., López-López, I., Jiménez- Colmenero, F., 2008c. Raman spectroscopic evaluation of meat batter structural changes induced by thermal treatment and salt addition. J. Agric. Food Chem. 56 (16), 7119–7124.

Herrero, A.M., Carmona, P., Cofrades, S., Jiménez-Colmenero, F., 2008d. Raman spectroscopic determination of structural changes in meat batters upon soy protein addition and heat treatment. Food Res. Int. 41 (7), 765–772.

Herrero, A.M., Carmona, P., Jiménez-Colmenero, F., Ruiz-Capillas, C., 2010. Applications of vibrational spectroscopy to study protein structural changes in muscle and meat batter systems. In: Chalmers, J., Griffiths, P., Li-Chan, E. (Eds.), Applications of Vibrational Spectroscopy to Food Science. John Wiley & Sons, New York, pp. 315–328.

Herrero, A.M., Carmona, P., Pintado, T., Jimenez-Colmenero, F., Ruiz-Capillas, C., 2012. Lipid and protein structure analysis of frankfurters formulated with olive oil-in-water emulsion as animal fat replacer. Food Chem. 135 (1), 133–139.

Herrero, A.M., Ruiz-Capillas, C., Jiménez-Colmenero, F., Carmona, P., 2014. Raman spectroscopic study of structural changes upon chilling storage of frankfurters containing olive oil bulking agents as fat replacers. J. Agric. Food Chem. 62 (25), 5963–5971.

Honikel, K.O., Hamm, R., 1994. Measurement of water-binding capacity and juiciness. In: Pearson, A.M., Dutson, T.R. (Eds.), Quality Attributes and Their Measurement in Meat, Poultry and Fish Products. Advances in Meat Research Series. Chapman and Hall, London, pp. 125–159.

Hoving-Bolink, A.H., Vedder, H.W., Merks, J.W.M., de Klein, W.J.H., Reimert, H.G.M., Frankhuizen, R., et al., 2005. Perspective of NIRS measurements early post mortem for prediction of pork quality. Meat Sci. 69 (3), 417–423.

Jiménez-Colmenero, F., Herrero, A.M., Cofrades, S., Ruíz-Capillas, C., 2016. Meat: eating quality and preservation. In: Caballero, B., Finglas, P.M., Toldra, F. (Eds.), Encyclopedia of Food and Health. Elsevier, pp. 685–692.

Kamruzzaman, M., ElMasry, G., Sun, D.W., Allen, P., 2012. Prediction of some quality attributes of lamb meat using near infrared hyperspectral imaging and multivariate analysis. Anal. Chim. Acta 714, 57–67.

Kamruzzaman, M., ElMasry, G., Sun, D.W., Allen, P., 2013a. Non-destructive assessment of instrumental and sensory tenderness of lamb meat using NIR hyperspectral imaging. Food Chem. 141 (1), 389–396.

Kamruzzaman, M., Makino, Y., Oshita, S., 2016a. Hyperspectral imaging for real-time monitoring of water holding capacity in red meat. LWT - Food Sci. Technol. 66, 685–691.

Kamruzzaman, M., Makino, Y., Oshita, S., 2016b. Online monitoring of red meat color using hyperspectral imaging. Meat Sci. 116, 110–117.

Kamruzzaman, M., Sun, D.W., ElMasry, G., Allen, P., 2013b. Fast detection and visualization of minced lamb meat adulteration using NIR hyperspectral imaging and multivariate image analysis. Talanta 103, 130–136.

Khodabux, K., L'Omelette, M.S., Jhaumeer-Laulloo, S., Ramasami, P., Rondeau, P., 2007. Chemical and near-infrared determination of moisture, fat and protein in tuna fishes. Food Chem. 102 (3), 669–675.

Krimm, S., Bandekar, J., 1986. Vibrational spectroscopy and conformation of peptides, polypeptides, and proteins. Adv. Protein Chem. 38, 181–365.

Kusualik, P.G., Mandy, M.E., Svishchev, I.M., 1994. The dielectric-constant of polar fluids and the distribution of the total dipole-moment. J. Chem. Phys. 100, 7654–7664.

Lafleur, M., Pigeon, M., Pézolet, M., Caillé, J.P., 1989. Raman spectrum of interstitial water in biological systems. J. Phys. Chem. C 93 (4), 1522–1526.

Larsson, K., 1976. Raman spectroscopy for studies of interface structure in aqueous dispersions. In: Paoleti, R., Jacini, G., Porcellati, R. (Eds.), Lipids: Technology. Raven Press, Michigan, pp. 355–360.

Larsson, K., Rand, R.P., 1973. Detection of changes in the environment of hydrocarbon chains by Raman spectroscopy and its applications to lipid-protein system. Biochim. et Biophys. Acta 326 (2), 245–255.

Levin, I.W., Lewis, E.N., 1990. Fourier transform Raman spectroscopy of biological materials. Anal. Chem. 62 (21), 1101A–1111A.

Li-Chan, E., 2010. Introduction to vibrational spectroscopy in Food science. In: Chalmers, J., Griffiths, P., Li-Chan, E. (Eds.), Applications of Vibrational Spectroscopy to Food Science. John Wiley & Sons, pp. 3–30.

Li-Chan, E.C.Y., 1996. The applications of Raman spectroscopy in food science. Trends Food Sci. Technol. 7 (11), 361–370.

Li-Chan, E.C.Y., Nakai, S., Hirotsuka, M., 1994. Raman spectroscopy as a probe of protein structure in food system. In: Yada, R.Y., Jackman, R.L., Smith, J.L. (Eds.), Protein Structure. Function Relationships in Foods. Blackie Academic and Professional, Chapman and Hall, London, pp. 163–197.

Liu, Y.L., Chen, Y.R., 2000. Two-dimensional correlation spectroscopy study of visible and near-infrared spectral variations of chicken meats in cold storage. Appl. Spectrosc. 54 (10), 1458–1470.

Liu, Y.L., Chen, Y.R., 2001. Two-dimensional visible/near-infrared correlation spectroscopy study of thawing behavior of frozen chicken meats without exposure to air. Meat Sci. 57 (3), 299–310.

Liu, Y., Chen, Y.R., Ozaki, Y., 2000. Two-dimensional visible/near-infrared correlation spectroscopy study of thermal treatment of chicken meats. J. Agric. Food Chem. 48 (3), 901–908.

Liu, Y., Lyon, B.G., Windham, W.R., Realini, C.E., Pringle, T.D.D., Duckett, S., 2003. Prediction of color, texture, and sensory characteristics of beef steaks by visible and near infrared reflectance spectroscopy. A feasibility study. Meat Sci. 65 (3), 1107–1115.

Liu, Y., Lyon, B.G., Windham, W.R., Lyon, C.E., Savage, E.M., 2004. Prediction of physical, color, and sensory characteristics of broiler breasts by visible/near infrared reflectance spectroscopy. Poultry Sci. 83 (8), 1467–1474.

Lu, X., Al-Qadiri, H.M., Lin, M., Rasco, B.A., 2011. Application of mid-infrared and Raman spectroscopy to the study of bacteria. Food Bioprocess Technol. 4 (6), 919–935.

Maeda, Y., Kitano, H., 1995. The structure of water in polymer systems as revealed by Raman spectroscopy. Spectrochim. Acta Part A 51A (14), 2433–2446.

Marechal, Y., 1991. Infrared-spectra of water.1. Effect of temperature and of H/D isotopic dilution. J. Chem. Phys. 95, 5565–5573.

McDonald, H., Bedwell, B., Gulari, E., 1986. FTIR spectroscopy of microemulsion structure. Langmuir 2 (6), 704–708.

McGlone, V.A., Devine, C.E., Wells, R.W., 2005. Detection of tenderness, post-rigor age and water status changes in sheep meat using near infrared spectroscopy. J. Near Infrared Spectrosc. 13 (5), 277–285.

Meisel, S., Stöckel, S., Rösch, P., Popp, J., 2014. Identification of meat-associated pathogens via Raman Microspectroscopy. Food Microbiol. 38, 36–43.

Muik, B., Lendl, B., Molina-Diaz, A., Ayora-Canada, M.J., 2005. Direct monitoring of lipid oxidation in edible oils by Fourier transform Raman spectroscopy. Chem. Phys. Lipids 134 (2), 173–182.

Naganathan, G.K., Grimes, L.M., Subbiah, J., Calkins, C.R., Samal, A., Meyer, G.E., 2008. Partial least squares analysis of near-infrared hyperspectral images for beef tenderness prediction. Sens. Instrum. Food Qual. Saf. 2 (3), 178–188.

Noda, I, 2007, 'Two-dimensional correlation analysis useful for spectroscopy, chromatography, and other analytical measurements', Analytical Sciences, vol. 23, no. 2, pp. 139–146.

Papadopoulou, O., Panagou, E.Z., Tassou, C.C., Nychas, G.J.E., 2011. Contribution of Fourier transform infrared (FTIR) spectroscopy data on the quantitative determination of minced pork meat spoilage. Food Res. Int. 44 (10), 3264–3271.

Park, B., Chen, Y.R., Hruschka, W.R., Shackelford, S.D., Koohmaraie, M., 1998. Near infrared reflectance analysis for predicting beef longissimus tenderness. J. Anim. Sci. 76 (8), 2115–2120.

Park, B., Yoon, S.C., Windham, W.R., Lawrence, K.C., Kim, M.S., Chao, K., 2011. Line-scan hyperspectral imaging for real-time in-line poultry fecal detection. Sens. Instrum. Food Qual. Saf. 5, 25–32.

Pedersen, D.K., Morel, S., Andersen, H.J., Engelsen, S.B., 2003. Early prediction of water-holding capacity in meat by multivariate vibrational spectroscopy. Meat Sci. 65 (1), 581–592.

Pelton, J.T., McLean, L.R., 2000. Spectroscopy methods for analysis of protein secondary structure. Anal. Biochem. 277 (2), 167–176.

Perisic, N., Afseth, N.K., Ofstad, R., Narum, B., Kohler, A., 2013. Characterizing salt substitution in beef meat processing by vibrational spectroscopy and sensory analysis. Meat Sci. vol. 95 (3), 576–585.

Phongpa-Ngan, P., Aggrey, S.E., Mulligan, J.H., Wicker, L., 2014. Raman spectroscopy to assess water holding capacity in muscle from fast and slow growing broilers. LWT - Food Sci. Technol. 57 (2), 696–700.

Prieto, N., Roehea, R., Lavín, P., Batten, G., Andrés, S., 2009. Application of near infrared reflectance spectroscopy to predict meat and meat products quality: a review. Meat Sci. 83 (2), 175–186.

Qu, J.H., Liu, D., Cheng, J.H., Sun, D.W., Ma, J., Pu, H., et al., 2015. Applications of near-infrared spectroscopy in food safety evaluation and control: A review of recent research advances. Crit. Rev. Food Sci. Nutr. 55 (13), 1939–1954.

Reid, L.M., O'Donnell, C.P., Downey, G., 2006. Recent technological advances for the determination of food authenticity. Trends Food Sci. Technol. 17 (7), 344–353.

Ripoche, A., Guillard, A.S., 2001. Determination of fatty acid composition of pork fat by Fourier transform infrared spectroscopy. Meat Sci. 58 (3), 299–304.

Ripoll, G., Alberti, P., Panea, B., Olleta, J.L., Sañudo, C., 2008. Near-infrared reflectance spectroscopy for predicting chemical, instrumental and sensory quality of beef. Meat Sci. 80 (3), 697–702.

Roza-Delgado, B., Soldado, A., Faria Oliveira, A.F.G., Martinez-Fernandez, A., Argamenteria, A., 2014. Assessing the value of a portable near infrared spectroscopy sensor for predicting

pork meat quality traits of "*Asturcelta autochthonous swine breed*". Food Anal. Methods 7 (1), 151–156.
Samuel, D., Park, B., Sohn, M., Wicker, L., 2011. Visible-near infrared spectroscopy to predict water-holding capacity in normal and pale broiler breast meat. Poult. Sci. 90 (4), 914–921.
Santos, M.I., Gerbino, E., Tymczyszyn, E., Gomez-Zavaglia, A., 2015. Applications of infrared and Raman spectroscopies to probiotic investigation. Foods 4 (3), 283–305.
Scheier, R., Scheeder, M., Schmidt, H., 2015. Prediction of pork quality at the slaughter line using a portable Raman device. Meat Sci. 103, 96–103.
Schrader, B., 1995. Infrared and Raman Spectroscopy. Methods and Applications. VCH Verlagsgesellschaft mbH, Weinheim.
Schweitzer-Stenner, R., 2006. Advances in vibrational spectroscopy as a sensitive probe of peptide and protein structure: a critical review. Vib. Spectrosc. 42 (1), 98–117.
Sedman, J., Ghetler, A., Enfield, A., Ismail, A.A., 2010. Infrared imaging: Principles and practices. In: Chalmers, J., Griffiths, P., Li-Chan, E. (Eds.), Applications of Vibrational Spectroscopy to Food Science. John Wiley & Sons, New York, pp. 109–131.
Shao, J.H., Zou, Y.F., Xu, X.L., Wu, J.Q., Zhou, G.H., 2011. Evaluation of structural changes in raw and heated meat batters prepared with different lipids using Raman spectroscopy. Food Res. Int. 44 (9), 2955–2961.
Shao, J.H., Deng, Y.M., Zhou, G.H., Xu, X.L., Liu, D.Y., 2015. A Raman spectroscopic study of meat protein/lipid interactions at protein/oil or protein/fat interfaces. Int. J. Food Sci. Technol. 50 (4), 982–989.
Surewicz, W.K., Mantsch, H.H., 1984. Infrared absortion methods for examining protein structure. In: Gruenwedel, D.W., Whitaker, J.R. (Eds.), Food Analysis. Principles and Techniques. Physicochemical Techniques. Marcel Dekker, pp. 135–162.
Thomas, G.J., 2002. New structural insights from Raman spectroscopy of proteins and their assemblies. Biopolymers 67 (4-5), 214–225.
Thyholt, K., Isaksson, T., 1997. Differentiation of frozen and unfrozen beef using near-infrared spectroscopy. J. Sci. Food Agric. 73 (4), 525–532.
Tu, A.T., 1982. Proteins. In: Tu, A.T. (Ed.), Raman Spectroscopy in Biology: Principles and Applications. John Wiley & Sons, New York, pp. 65–116.
Tu, A.T., 1986. Peptide backbone conformation and microenvironment of protein side-chains. In: Clark, R.J.H., Hester, R.E. (Eds.), Spectroscopy of Biological Systems. John Wiley and Sons, New York, pp. 47–112.
Tuma, R., 2005. Raman spectroscopy of proteins: from peptides to large assemblies. J. Raman Spectrosc. 36 (4), 307–319.
Uddin, M., Okazaki, E., 2004. Classification of fresh and frozen-thawed fish by near-infrared spectroscopy. J. Food Sci. 69 (8), 665–668.
van de Voort, F.R., Ismail, A.A., Sedman, J., Emo, G., 1994. Monitoring the oxidation of edible oils by Fourier transform infrared spectroscopy. J. Am. Oil Chem. Soc. 71 (3), 243–253.
van de Voort, F.R., Sedman, J., Russin, T., 2001. Lipids analysis by vibrational spectroscopy. Eur. J. Lipid Sci. Technol. 103 (2), 815–840.
Venel, C., Mullen, A., Downey, G., Troy, D., 2001. Prediction of tenderness and other quality attributes of beef by near infrared reflectance spectroscopy between 750 and 1100 nm; further studies. J. Near Infrared Spectrosc. 9 (3), 185–198.
Verma, S.P., Wallach, D.F.H., 1977. Changes of Raman scattering in the CH stretching region during thermally induced unfolding of ribonuclease. Biochem. Biophys. Res. Commun. 74, 473–479.

Walrafen, G.E., Fisher, M.R., 1986. Low-frequency Raman scattering from water and aqueous solutions: a direct measure of hydrogen bonding. Methods Enzymol. 127, 91–105.

Wang, Q., Lonergan, S.M., Yu, C., 2012. Rapid determination of pork sensory quality using Raman spectroscopy. Meat Sci. 91 (3), 232–239.

Williams, W., 1983. Estimation of protein secondary structure from the laser Raman amide I spectrum. J. Mol. Biol. 166, 581–603.

Windham, W., Smith, D., Berrang, M., Lawrence, K., Feldner, P., 2005. Effectiveness of hyperspectral imaging system for detecting cecal contaminated broiler carcasses. Int. J. Poult. Sci. 4 (9), 657–662.

Wold, J.P., Isaksson, T., 1997. Non-destructive determination of fat and moisture in whole Atlantic salmon by near-infrared diffuse spectroscopy. J. Food Sci. 62 (4), 734–736.

Xiong, Z., Xie, A., Sun, D.W., Zeng, X.A., Liu, D., 2015. Applications of hyperspectral imaging in chicken meat safety and quality detection and evaluation: A review. Crit. Rev. Food Sci. Nutr. 55 (9), 1287–1301.

Xu, X.L., Han, M.Y., Fei, Y., Zhou, G.H., 2011. Raman spectroscopic study of heat-induced gelation of pork myofibrillar proteins and its relationship with textural characteristic. Meat Sci. 87 (3), 159–164.

Zamora-Rojas, E., Perez-Marin, D., De Pedro-Sanz, E., Guerrero-Ginel, J.E., Garrido-Varo, A., 2012. Handheld NIRS analysis for routine meat quality control: Database transfer from at-line instruments. Chemometric Intell. Lab Syst. 114, 30–35.

Zanotti, J.M., Bellissent-Funel, M.C., Chen, S.H., 1999. Relaxational dynamics of supercooled water in porous glass. Phys. Rev. E 59 (3), 3084–3093.

Zhao, M., Downey, G., O'Donnell, C.P., 2015. Dispersive Raman spectroscopy and multivariate data analysis to detect offal adulteration of thawed beef burgers. J. Agric. Food Chem. 63 (5), 1433–1441.

Zou, M.Q., Zhang, X.F., Qi, X.H., Ma, H.L., Dong, Y., Liu, C.W., et al., 2009. Rapid authentication of olive oil adulteration by Raman spectrometry. J. Agric. Food Chem. 57 (14), 6001–6006.